

Wind Tunnel Measurements of Transonic Aerodynamic Loads on Mine Clearing Darts

Kennard Watson¹

Naval Surface Warfare Center – Panama City, FL

Ralph Carmichael², Dan Lesieutre², Marnix Dillenius³
Nielsen Engineering and Research, Inc, Mountain View, CA

Kevin Losser⁴, William Dietz⁵
Digital Fusion Solutions, Inc, Huntsville, AL

Michael Dean Neaves⁶
Naval Surface Warfare Center – Panama City FL

and

Christopher Hovland⁷
Naval Surface Warfare Center – Indian Head, MD

Wind tunnel tests were performed to measure the freestream and interference loads on multiple 6-inch long darts at speeds of Mach 0.8 to 1.2. The darts are intended for use in new mine clearance technology being developed by the U.S. Navy to support military amphibious operations. Freestream data were collected for a single dart at angles of attack up to 42 degrees, and interference data were collected for a dart in the presence of dart clusters. The interference results show the presence of significant interference loads when the bodies are in close proximity at transonic speeds. In addition to well-known drafting effects when the darts are placed behind each other, they also experience significant transverse interference forces when placed side-by-side. The force and moment data are in generally good agreement with semi-empirical and computational fluid dynamics models. This study fills a gap in published data for aerodynamic loads on multiple bodies in proximate flight at transonic speeds.

I. Introduction

THE Office of Naval Research is developing new technology to clear mines in support of amphibious operations by U.S. Marine Corps forces. The concept involves the use of precision strike weapons fired from naval guns or deployed from aircraft. The weapon carries a payload of hundreds of darts and flies a guided trajectory to the target mine belt, located on the beach or in the surf zone. The guidance system orients the weapon vertically above the target, and the dart payload is spin-dispensed to produce a circular impact pattern. Dispense occurs several hundred feet above the target at a transonic speed of about Mach 1.2.

Previous research suggests that the size of the dart impact pattern is sensitive to aerodynamic interference among the darts.¹ Predictions from computational fluid dynamics (CFD) models show that, when the darts are side-by-side

¹ Research Engineer, Automation and Dynamics Branch, Code HS15.

² Senior Research Engineer, Senior Member AIAA.

³ President, Associate Fellow AIAA.

⁴ Engineer, Member AIAA.

⁵ Director, Engineering Analysis, Member AIAA.

⁶ Research Engineer, Automation and Dynamics Branch, Code HS15, Senior Member AIAA.

⁷ Research Engineer, Propulsion Branch, Code E3130.

in close proximity, transverse interference forces drive the darts apart, generating patterns that are larger than would be expected from the launch kinematics (release altitude, speed, spin rate). This is a concern because large patterns are associated with lower dart density, resulting in reduced effectiveness in clearing mines.

Aside from numerous store-interference studies of weapons released from aircraft,^{2,3} experimental results are lacking on transonic aerodynamic loads of multiple bodies in close proximity. The test program described herein fills this data gap. Measured forces and moments are presented for darts in freestream conditions and in close proximity at speeds of Mach 0.8 to 1.2. The data are compared with predictions from an engineering-level method and a CFD model. Included are CFD predictions of a 183-dart dispense.

II. Materials and Methods

The wind tunnel test considered three dart geometries shown in Fig. 1. The tri-finned cylindrical dart is 6.49 inches long and 0.4875 inches diameter, with a blunt nose to provide stability during water and sand entry. The dart weighs 55 gm, and the center of gravity is 2.09 inches from the nose. Fin span is 0.19 inches and fin chord is 1.0 inch. Also shown in Fig. 1 is a finless version of this dart and a shortened version with a length of 3.25 inches.

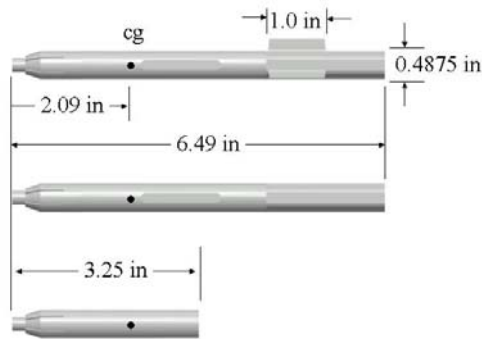


Figure 1. Schematic of the tri-finned dart and two finless versions.

Operationally, the finned darts are packaged into a BLU-109 Joint Direct Attack Munition (JDAM), shown in Fig. 2. The payload section contains 4735 darts packaged into nine stacks. There are no bulkheads between stacks, so the darts are in nose-to-tail contact. Side-by-side packaging is enabled by using two types of darts, one with forward-mounted tail fins and the other with aft-mounted fins. The aft-fin version was not included in the test.

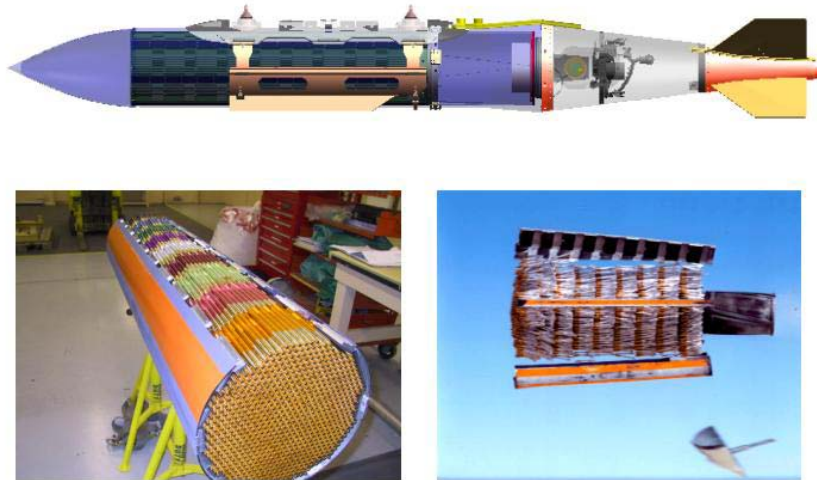


Figure 2. Flight test configuration showing BLU-109 JDAM delivery vehicle and dart payload (packaged and in flight).

The test was performed in the Transonic Tunnel 4T at Arnold Engineering Development Center. The test section is 12.5 ft long and has a square cross-section with a side dimension of 4 ft. It has a speed range of Mach 0.2 to 2.0. This facility has been used extensively for store integration work on fighter aircraft. Figure 3 shows the mounting arrangement for the dart freestream tests, and Fig. 4 shows the configuration for the interference tests, consisting of an instrumented dart, two finless and non-instrumented “dummy” darts, and a blunt-nose centerbody. The dummy darts were mounted to the centerbody at three radial locations and a circumferential position such that, when the metric dart is directly in between the two dummy darts, all of the bodies are equidistant from each other. The three offsets are 0.1, 0.2, and 0.4 inches, defined in Fig. 5 by the distance h between the surfaces of the dart and centerbody (0=surfaces in contact). The dummy darts were located axially such that the dart nose was aligned with the centerbody nose. The purpose of the centerbody is to simulate the payload when the darts are close together shortly after dispense (Fig. 2). This configuration was selected based on CFD modeling, which showed that the largest interference loads occur for darts on the perimeter of the payload, with the interior darts acting collectively as a blunt body. Two centerbody sizes were tested: 3-inch diameter and 5-inch diameter. The centerbody and dummy darts were at zero angle of attack for the majority of the tests.

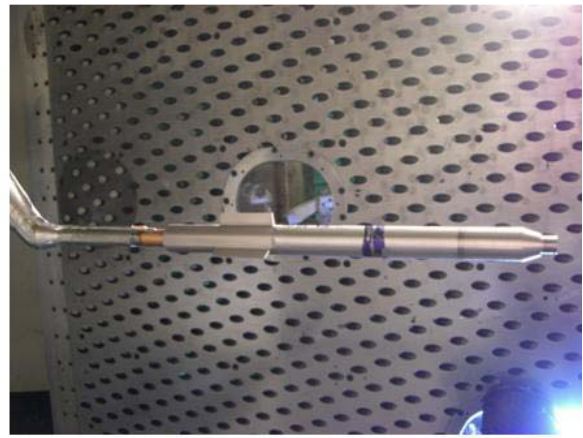
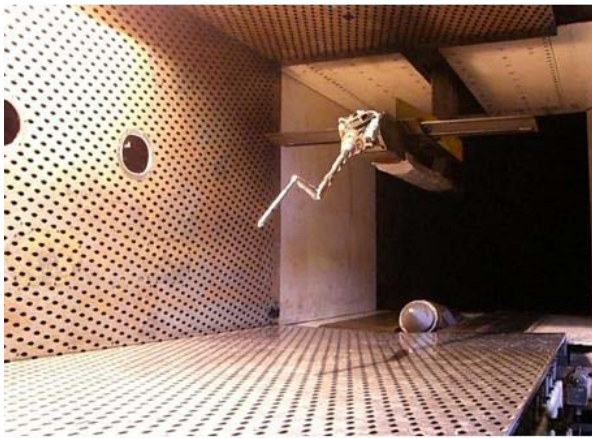


Figure 3. Freestream test mounting arrangement.

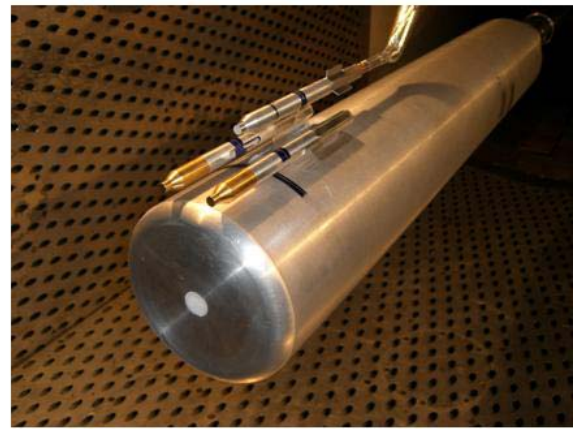


Figure 4. Interference test mounting arrangement (5-inch diameter centerbody shown).

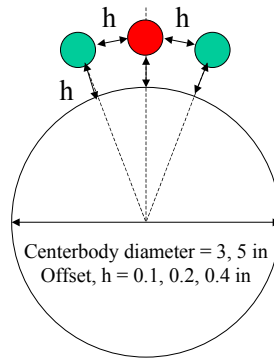


Figure 5 - Definition of dummy dart radial offset.

Figure 6 shows sign conventions for the dart aerodynamic coefficients and flow angles. The force coefficients are referenced to the dart cross-section area, and the moment coefficients are referenced to the dart cross-section area and diameter. The reference center for the moment coefficients is the dart center of gravity, 2.09 inches behind the nose.

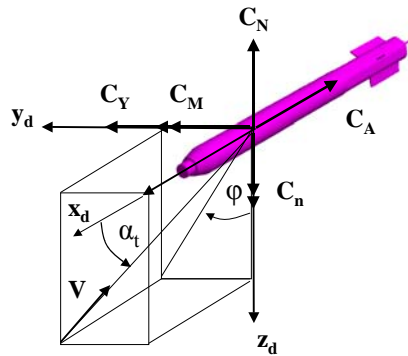


Figure 6 - Sign conventions for aerodynamic coefficients and flow angles.

For all of the tests, forces and moments were measured on a single instrumented dart – one of the three configurations in Fig. 1 – attached to the captive trajectory system (CTS), enabling the dart to be positioned at an arbitrary location in the tunnel with high precision. The dart was fitted to an internal six-component strain gauge balance with a diameter of 0.3 inches. The axial force measurements were not corrected for base pressure due to the small size of the model relative to the sting attachment, allowing no room for a pressure probe.

The majority of the testing was performed at Mach numbers of 0.8 and 1.2, although some tests were conducted at Mach 0.5. For the interference measurements, the nominal stagnation pressure was set to 1200 psf, and the nominal unit Reynolds number was 2.5 million per foot at Mach 1.2 and 2.25 million per foot at Mach 0.8. For the freestream measurements, the stagnation pressure was reduced to 800 psf at Mach 0.8 and 1000 psf at Mach 1.2 in order to remain within the load limits of the balance when the dart was at high angles of attack. The corresponding Reynolds numbers were 1.5 and 2.1 million per foot.

The force and moment data were compared with two prediction methods. The Engineering Level Method for Darts alone and in presence of a Dispenser (ELMDD) is a semi-empirical model that combines linear theory with discrete vortex methods to predict aerodynamic loads at high angles of attack.⁴ High angle-of-attack capability is provided by the MISL3 module, which has been incorporated into ELMDD and includes a method to predict the onset and magnitude of out-of-plane forces and moments,⁵ referred to as “phantom yaw” effects. OVERFLOW-2 is a Navier-Stokes solver developed for the Department of Defense under the Common High Performance Computing Software Initiative.^{6,7} Predictions from OVERFLOW-2 and ELMDD have been incorporated into a six degree-of-freedom (6-DOF) simulation program that predicts the trajectories of darts dispensed from a guided vehicle.¹

The OVERFLOW-2 predictions in the following section use 18 million grid points in 23 grids to represent the wind tunnel model. This number includes off-body grids as well as near-body grids for each dart. Each finless dart consisted of five grids with a near-wall grid spacing of 5×10^{-6} ft. A total of approximately 916,000 grid points were used for each dart. The grid system was constructed with the dummy darts free floating above the parent body. Not included in the grid system were struts holding the dummy darts to the centerbody or the sting attached to the metric dart. Also, the wind tunnel walls were not modeled. The axial force on the dart was calculated with and without the effect of base drag, which was excluded by integrating the force over the entire dart surface except for the base. Neglecting the base of the dart simulates the effect of the sting attachment.

III. Results

This section presents a portion of the freestream and interference load data collected on the metric dart at Mach numbers of 0.8 and 1.2. Freestream data consider the finned dart at zero roll angle and angles of attack between ± 42 deg. The interference data consider the 6.49-inch finless metric dart for both centerbody geometries. No results are shown for the 3.25-inch finless variant. The test report contains the complete set of the wind tunnel data.⁸

Figures 7-9 compare freestream measurements for the finned dart with ELMDD and OVERFLOW-2 predictions. The axial force data shown in Fig. 7 were not corrected for base pressure; therefore, the model predictions are shown with and without the effect of base drag. Comparing the data with the no-base predictions at Mach 0.8, the measured CA values are underpredicted by ELMDD and slightly overpredicted by OVERFLOW-2. At Mach 1.2, the no-base CFD predictions are in good agreement with the data and underpredicted by ELMDD. For the semi-empirical axial force prediction within ELMDD, the body nose was modeled as hemispherical which is an approximation of the actual truncated button nose. For supersonic flow with a detached bow shock, this is a reasonable approximation. For transonic flow, the approximation likely underpredicts transonic wave drag.

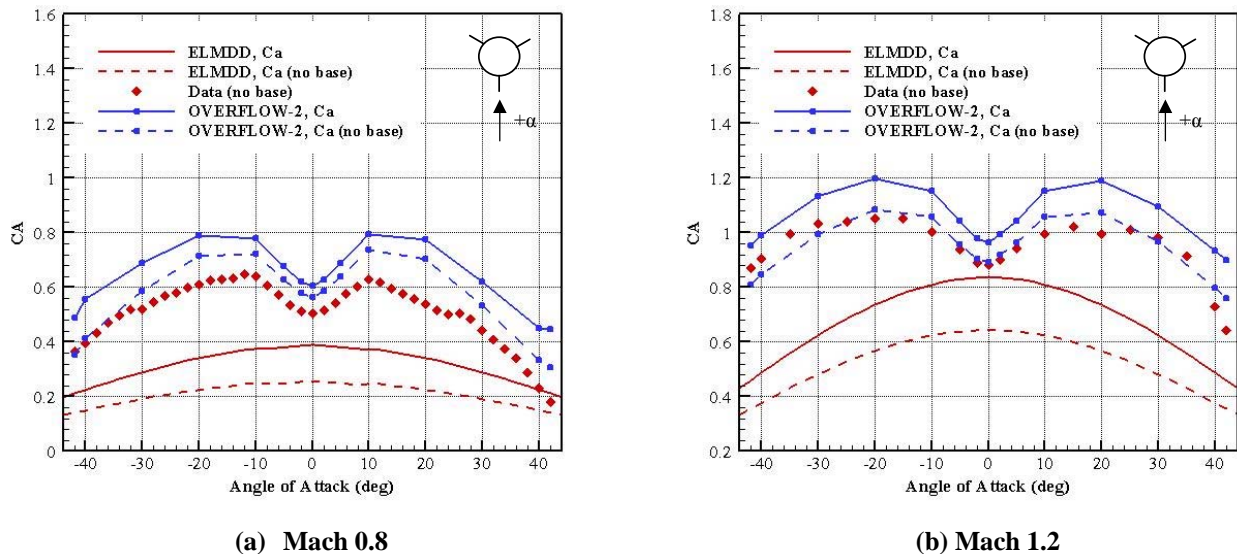
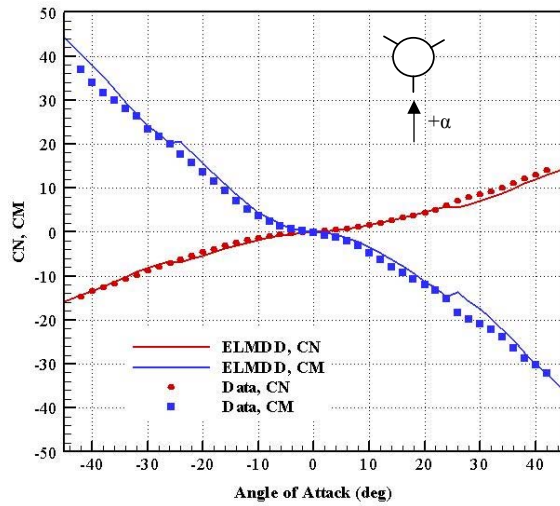
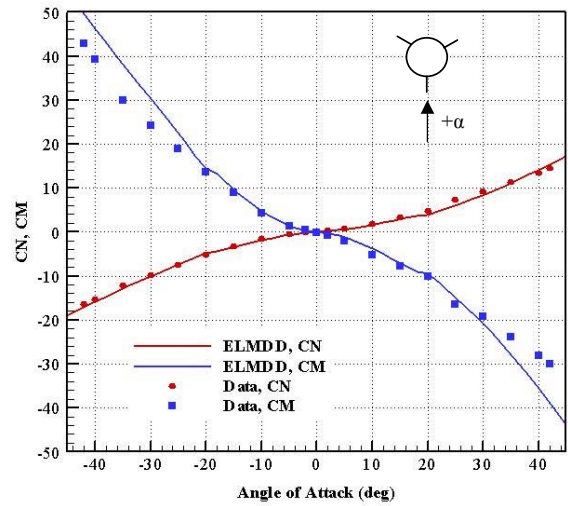


Figure 7. Freestream axial force coefficients versus angle of attack on the finned dart at zero roll and Mach 0.8 and 1.2.

Figure 8 shows the normal force and pitch moment comparisons. ELMDD is in excellent agreement with the data except for angles of attack above ± 30 deg, where the model overpredicts the magnitude of the pitch moment. The “jump” in normal force in the Mach 0.8 predictions at $\alpha \sim 24$ deg is due to the crossflow drag component of the body force switching from laminar to turbulent. Not shown in this figure are the OVERFLOW-2 predictions, which essentially overlap the ELMDD results except at high angles of attack, where the CFD predictions are in better agreement with the data.



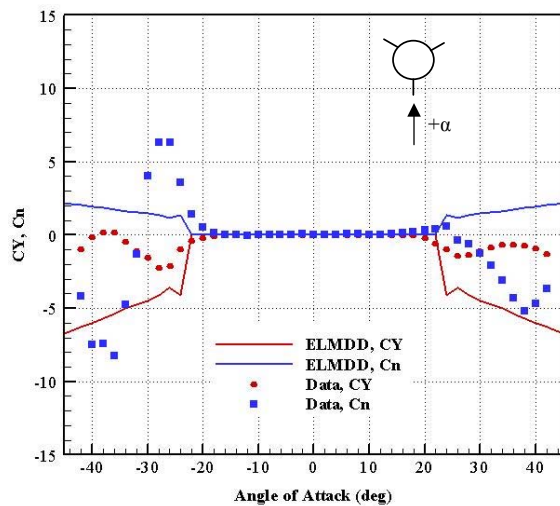
(a) Mach 0.8



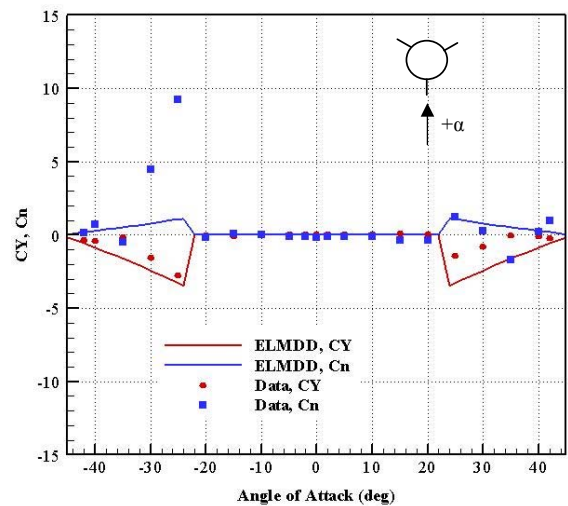
(b) Mach 1.2

Figure 8. Freestream normal force and pitch moment coefficients versus angle of attack on the finned dart at zero roll and Mach 0.8 and 1.2.

Figure 9 shows the measured and predicted out-of-plane side force and yaw moment for zero sideslip. ELMDD models only the “phantom yaw” associated with the forebody; it does not include any effects of asymmetric forebody vorticity influencing the fin section. The magnitude of phantom side force (and its center of pressure) predicted for the forebody by the present version of ELMDD is the maximum amount to be expected. The angle of attack where the phantom side force is first seen is predicted well for both Mach 1.2 and 0.8. OVERFLOW-2 predicts zero steady side force and yaw moment for these flow conditions.



(a) Mach 0.8



(b) Mach 1.2

Figure 9. Freestream side force and yaw moment coefficients versus angle of attack on the finned dart at zero roll and Mach 0.8 and 1.2.

Figures 10 and 11 show the interference normal force and pitch moment coefficients at Mach 1.2 on the finless metric dart in the presence of the centerbody and two dummy darts offset radially at 0.1 inches. All of the bodies are at the same axial position, the nose positions of the darts are in-line with the centerbody, and all are at zero angle of

attack. The CN and CM values are shown as a function of radial offset h of the metric dart from the centerbody, nondimensionalized by the dart diameter. Positive CN is toward the centerbody, and positive CM is nose toward the centerbody. In general, OVERFLOW-2 is in good agreement with the data. The predictions show a slight discrepancy in normal force and pitch moment coefficients when the metric dart is in close proximity to the centerbody. At this position, the metric dart is at its closest proximity to the dummy darts as well. As the metric dart's radial offset increases, the normal force coefficient follows the trend of the wind tunnel data. Figure 12 shows predicted surface pressures for the metric dart at a height of 0.4 inches.

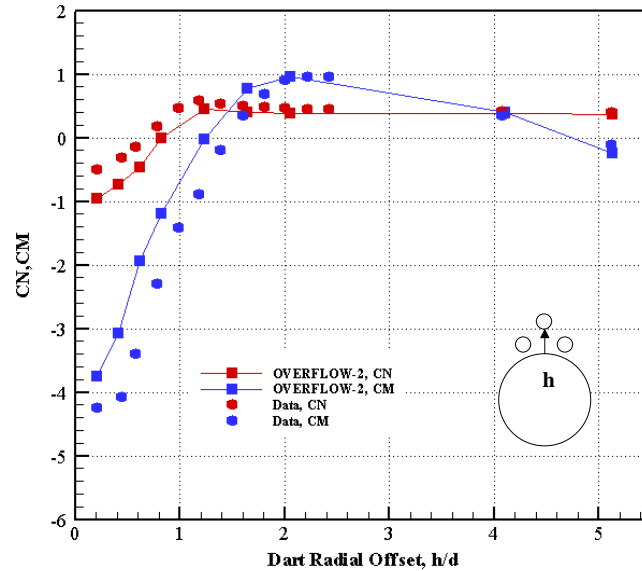


Figure 10. Interference normal force and pitch moment coefficients on the finless dart versus radial offset at Mach 1.2 for a 3-inch centerbody and two dummy darts offset 0.1 inches.

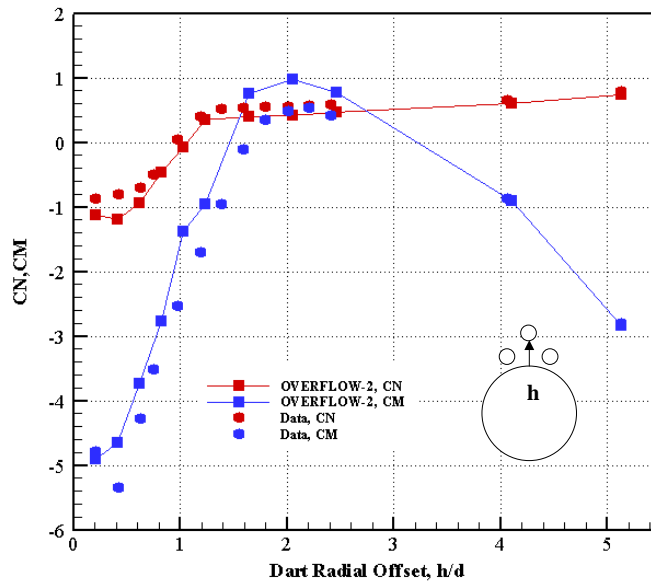


Figure 11. Interference normal force and pitch moment coefficients on the finless dart versus radial offset at Mach 1.2 for a 5-inch centerbody and two dummy darts offset 0.1 inches.

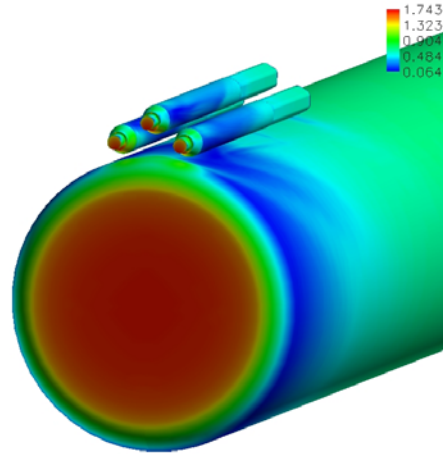


Figure 12. Predicted surface pressures on the 5-inch centerbody with two dummy darts offset 0.1 inches and the finless dart offset 0.4 inches, Mach 1.2.

Figures 13 and 14 show measured and predicted axial force coefficients on the finless metric dart in a drafting position behind one of the dummy darts mounted on the large centerbody. For these comparisons, each dummy dart was at a radial offset of 0.4 inches from the 5-inch centerbody. Axial force coefficients are shown versus the axial distance between the base of the dummy dart and nose of the metric dart, nondimensionalized by dart length. Results are presented for the metric dart directly behind the dummy dart (Fig. 13) and offset radially by one dart diameter from the dummy (Fig. 14). Note that dart offset is the radial separation between the dart surfaces, not their centerlines. OVERFLOW-2 predictions show an asymptotic behavior up to an axial separation of about 2.5 dart lengths. Beyond this location, the metric dart is in the presence of an expansion wave as the centerbody diameter reduces from 5 inches to 3 inches in order to attach to the sting hardware. Figure 15 shows a Mach number plot that is representative of the flow field for the drafting configuration.

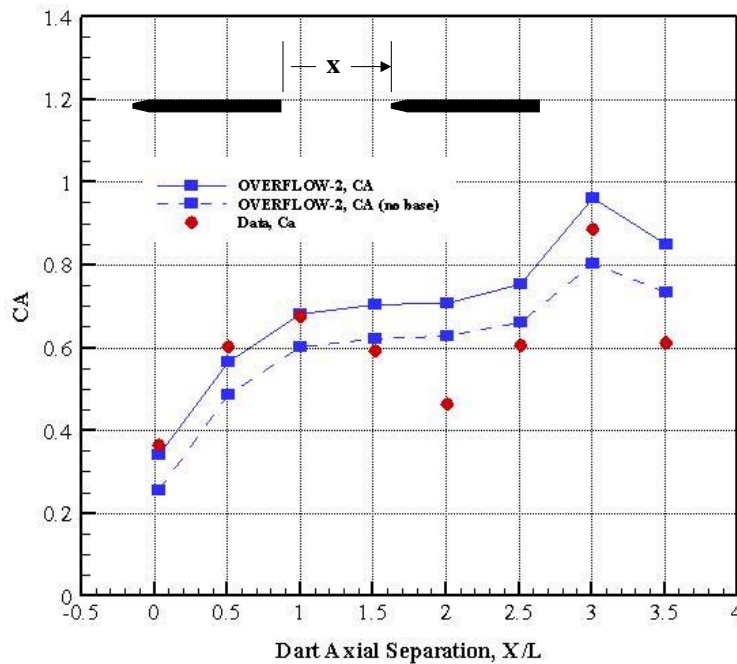


Figure 13. Axial force coefficients on the finless dart versus axial position at Mach 1.2 for a 5-inch centerbody and two dummy darts offset 0.4 inches and metric dart directly behind dummy.

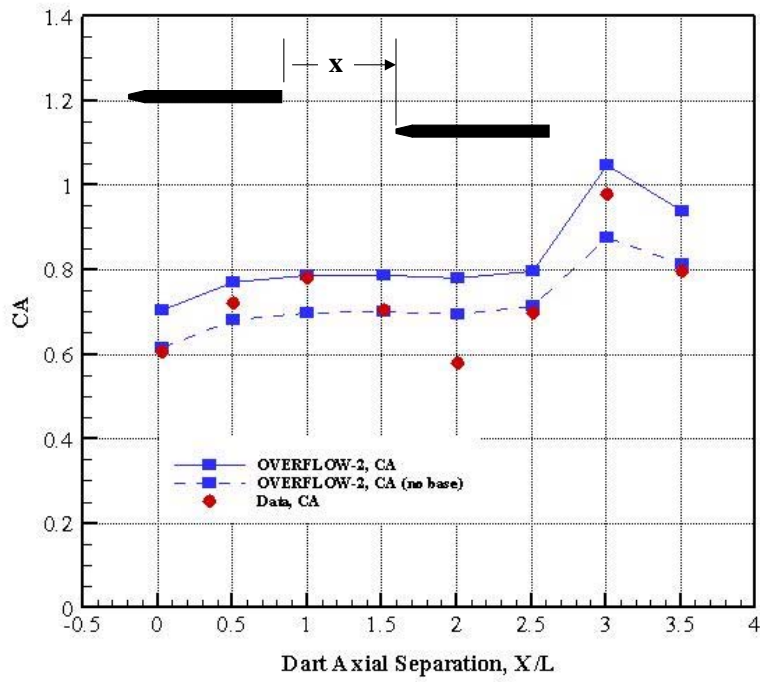


Figure 14. Axial force coefficients on the finless dart versus axial position at Mach 1.2 for a 5-inch centerbody and two dummy darts offset 0.4 inches and metric dart offset one diameter (note that radial offset corresponds to the distance between dart surfaces, not centerlines).

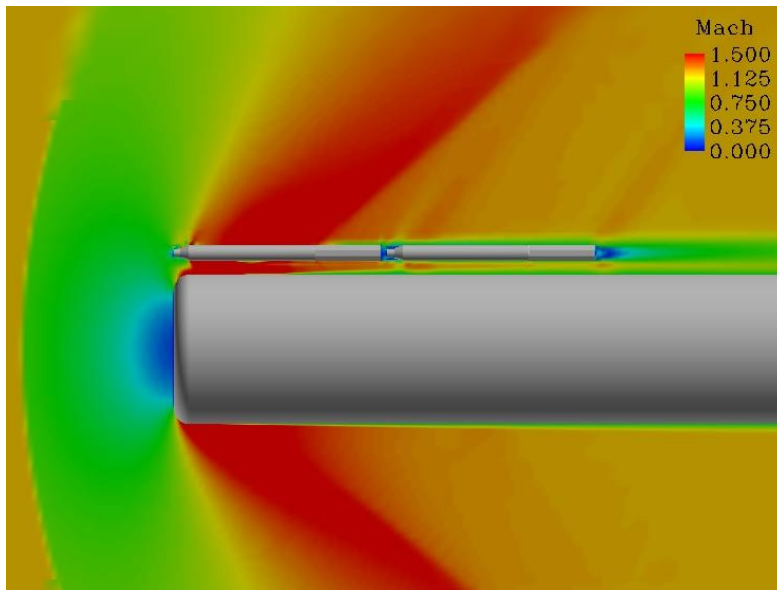


Figure 15. Side view of predicted Mach number field for a 5-inch centerbody with finless dart directly behind dummy dart, Mach 1.2.

IV. Discussion

Flight tests of the system shown in Fig. 2 revealed a larger dart impact pattern than expected based on the release conditions.¹ CFD analysis and 6-DOF trajectory predictions showed that the size of the pattern is sensitive to dart-on-dart aerodynamic interference occurring shortly after dispense at transonic speeds.¹ OVERFLOW-2 predictions indicate the presence of large transverse interference loads when the darts are in very close proximity, generally within about 1-2 diameters of each other. This effect is evident in the comparisons shown in Figs. 10 and 11. The metric dart experiences a large expulsive normal force and nose-out pitching moment when it is within one diameter of the centerbody and dummy darts. The effect diminishes rapidly with radial distance.

After validating OVERFLOW-2 calculations using the wind tunnel data, multiple-dart dispense simulations were performed for groups of darts. OVERFLOW-2 simulations with collision detection and subsequent rigid-body reaction impulse algorithms⁹ provide insight into the chaotic initial dispense phase. A time step convergence study on a single dart was performed to provide an acceptable physical timestep and the required number of dual-time subiterations. Figure 16 shows three stacks of 183 darts packaged in nose-to-tail contact similar to the deployment concept in Fig. 2. Pressure contours are shown for the dart payload at Mach 1.2, and the overset grid system can be seen in the centerline cut plane. This packaging scheme results in significant contact between the darts and a large number of interpolation orphans. For tractability reasons, the calculations were performed without collar grids in dart-on-dart contact regions. The averaging of neighbor values into orphan regions should provide reasonable property values during dart-on-dart contact. To enhance flow solver robustness with touching and colliding darts (and subsequent overset interpolation orphans), single fringes and the Spalart-Allmaras turbulence model are used for multiple-dart 6-DOF analysis.

The 6-DOF initial conditions were established by a steady-state run followed by a prescribed motion spin of 180 deg at 12 Hz spin rate. Figure 17 shows the dispense pattern after approximately 50 ms. Steady calculations for the initial packing of darts predicted an outward radial force for the front outer layer, and the OVERFLOW-2 6-DOF dispense calculations appears to show the front outer layer being preferentially ejected from the spinning pack of darts. The rear stacks do not have the large aerodynamic outward radial force and experience a kinematic dispense until significant nose-to-tail collisions begin to occur. The nose-to-tail collisions between the rear and front stacks generate large angles of attack on individual darts. The aerodynamic forces from the large angles of attack are significantly larger than the actual collision forces and may be an important pattern size driver. The large angle of attack darts are ultimately ejected from the pack and tend to increase pattern size.

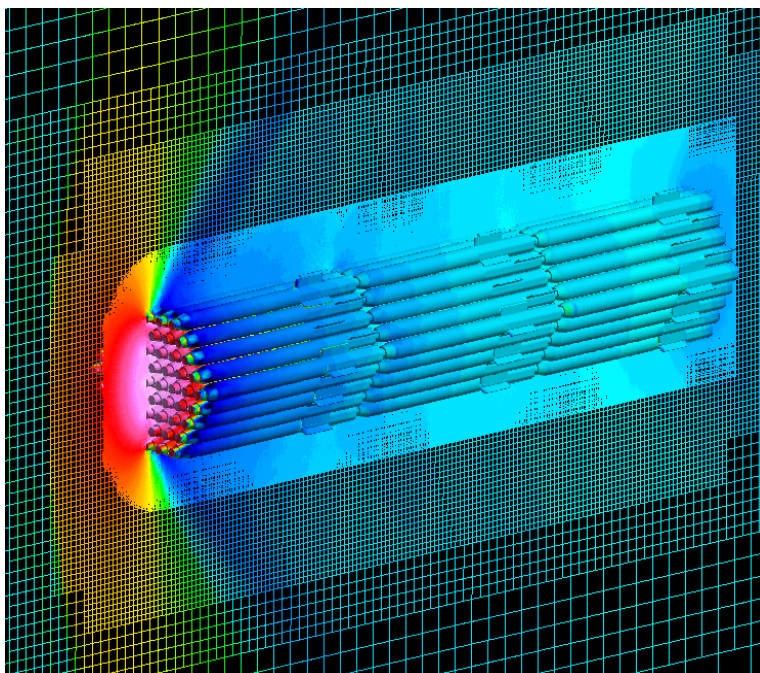


Figure 16. OVERFLOW-2 simulation of 183 darts in packaged configuration at Mach 1.2.

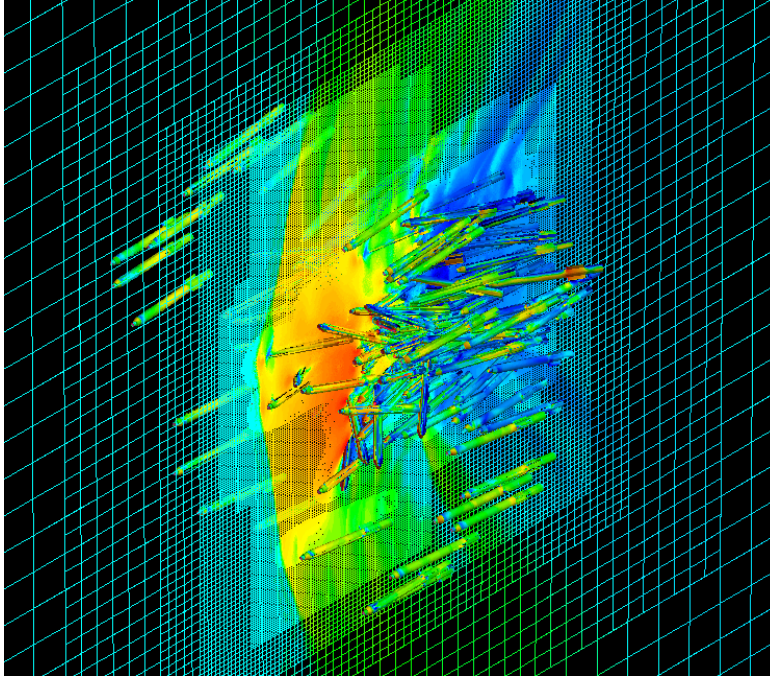


Figure 17. OVERFLOW-2 simulation of 183 darts 50 ms after release at Mach 1.2.

V. Conclusion

This test measured the aerodynamic loads on a dart in freestream conditions and in the presence of other darts and a centerbody representing a swarm of darts. Measurements were performed on finned and finless versions of the dart at Mach 0.8 and 1.2. OVERFLOW-2 was shown to accurately predict the transverse interference forces and moments of darts in close proximity at transonic speeds. The validated CFD model is being used to investigate the effect of dispense speed, spin rate, and packaging on the dynamics of large payloads of darts released from a guided missile.

Acknowledgments

The Office of Naval Research, Code 321OE (Brian Almquist), funded the wind tunnel test and the aerodynamic analysis presented in this paper. The authors appreciate the assistance provided by Mickey Kiber of Arnold Engineering Development Center.

References

- ¹ Watson, K. P., Neves, M. D., and Nguyen, T. C. "Development of a 6-DOF Model for Mine Clearing Darts," AIAA 2006-0672, 45th AIAA Aerospace Sciences Meeting, Reno, NV, January 2006.
- ² Dillenius, M. F. E., Lesieutre, D. J., Perkins, S. C., Jr., and Love, J. F., "Prediction of Nonlinear Missile Aerodynamics with Applications Including Store Separation," RTO-MP-5, /Missile Aerodynamics/, Nov. 1998.
- ³ Dillenius, M. F. E., Perkins, S. C., Jr., Carmichael, R. L., and Lesieutre, D. J., "Continued Development of the Engineering-Level Method (ELM) for Dart Dispense Aerodynamic Modeling," NEAR TR 609, Nielsen Engineering & Research, Mountain View, CA, Oct. 2004.
- ⁴ Lesieutre, D. J., Love, J. F., Dillenius, M. F. E., and Blair, A. B. Jr., "Recent Applications and Improvements to the Engineering-Level Aerodynamic Prediction Software MISL3," AIAA 2002-0275, 40th AIAA Aerospace Sciences Meeting, Reno, NV, January 2002.
- ⁵ Ericsson, L.E. and Reding, J.P., "Asymmetric Vortex Shedding from Bodies of Revolution," in Tactical Missile Aerodynamic, ed. Hemsch, M.J. and Nielsen, J.N., AIAA, 1986, pp. 243-296.
- ⁶ Nichols, R., Tramel, R., and Buning, P., "Solver and Turbulence Model Upgrades to OVERFLOW 2 for Unsteady and High-Speed Applications," AIAA-2006-2824, June 2006.

⁷ Meakin, R. and Wissink, A., “*Unsteady Aerodynamic Simulation of Static and Moving Bodies Using Scalable Computers*,” AIAA 99-3302-CP, 14th AIAA CFD Conference, Norfolk, VA, July 1999.

⁸ Carmichael, R. L. and Dillenius, M. F. E., “*Measurements of Transonic Aerodynamic Interference Between Mine Clearing Darts*,” NEAR TR 638, Nielsen Engineering & Research, Mountain View, CA, Dec. 2007.

⁹ Meakin, R. L., “*A General Simulation Method for Multiple Bodies in Proximate Flight*,” AIAA-2003-3831, 16th AIAA Computational Fluid Dynamics Conference, June 2003.